ACTA IMEKO
ISSN: 2221-870X
September 2023, Volume 12, Number 3, 1 - 6

Concept and preliminary design of dielectric resonator for anisotropic measurement of the surface impedance

Kostiantyn Torokhtii[1], Andrea Alimenti[1], Pablo Vidal García[1], Nicola Pompeo[1], Enrico Silva[1]

[1] *Dept. of Industrial, Electronic and Mechanical Engineering, Roma Tre University, Via Vito Volterra 62, 00146 Rome, Italy*

ABSTRACT
The surface impedance of superconductors as a function of intense (~ 10 T) static magnetic field at varying orientations with respect to the crystallographic axes is of large interest for both characterization purposes, in view of the material engineering, and from the point of view of devices to be used in fundamental physics experiments. A varying field orientation is customarily obtained with mechanically rotating magnets, whose complexity limits the attainable maximum fields to a few T. Here we propose a special proof of concept design for a measuring cell in which the magnetic field orientation is fixed, while the sample orientation can be changed through its incorporation in a rotating portion of the cell. The main design choices are thus proposed for the measuring cell: a cylindrical dielectric loaded resonator, to be used within the surface perturbation approach for the measurement of the surface impedance of flat samples with typical size 10 × 10 mm^2. The main focus in this preliminary work is put on the sensitivity attainable on the surface resistance, i.e. the real part of the surface impedance.

Section: RESEARCH PAPER

Keywords: surface impedance measurement; dielectric loaded resonator; microwave characterization of superconductors

Citation: Kostiantyn Torokhtii, Andrea Alimenti, Pablo Vidal García , Nicola Pompeo, Enrico Silva, Concept and preliminary design of dielectric resonator for anisotropic measurement of the surface impedance, Acta IMEKO, vol. 12, no. 3, article 24, September 2023, identifier: IMEKO-ACTA-12 (2023)-03-24

Section Editor: Jan Saliga, Technical university of Kosice, Slovakia, Jakub Svatos, CVUT Prague, Czech Republic, Platon Sovilj, University of Novi Sad, Serbia

Received January 10, 2023; **In final form** June 12, 2023; **Published** September 2023

Corresponding author: Kostiantyn Torokhtii, e-mail: kostiantyn.torokhtii@uniroma3.it

1. INTRODUCTION

Measurements of the surface impedance Z_S of superconductors in high magnetic fields with varying orientations are of specific but strong interest. Indeed, the most promising superconductors for the realization of next generation high field magnets, in applications such as high definition Nuclear Magnetic Resonance (NMR) [1] and future compact fusion reactors [2], are anisotropic. Hence, angle dependent surface impedance is a useful characterization tool for the material engineering process. Moreover, large physics experiments, such as the Future Circular Collider [3] and the hunt for Dark Matter [4], require low surface impedance superconductors to be operated in high magnetic fields applied at various orientations with respect to the crystallographic axes. A standard approach in surface impedance measurements is based on the dielectric-loaded resonator (DR) [5]. Indeed, the dielectric loaded resonator method is the most sensitive technique for Z_S measurements in a wide range of temperatures and magnetic fields [5], [6], [7].

Usually, the measurement cell is simply a Hakki-Coleman DR [8], where a cylindrical dielectric puck is coaxially placed within a cylindrical conducting enclosure. In the commonly used surface perturbation technique, the sample replaces one of the conducting flat surfaces of the cavity. By changing an external parameter, such as the dc magnetic field intensity H, the induced variations "Δ" of the real (R_S) and imaginary (X_S) parts of Z_S with respect to a reference value $Z_{S,ref} = Z_S(H = H_{ref})$, can be derived from the measurement of the DR quality factor Q and resonant frequency f_0, respectively [9], [10], [11]:

$$\Delta R_S + i\Delta X_S = G_S\left(\Delta\frac{1}{Q} - 2i\frac{\Delta f_0}{f_0}\right) - \text{background}, \quad (1)$$

where the geometrical factor of the sample G_S is a constant analytically computed or determined through electromagnetic simulations; the term "background" refers to other DR contributions that can be removed by a proper calibration procedure [10]. After some simple calculations, the sensitivity on R_S and X_S is obtained:

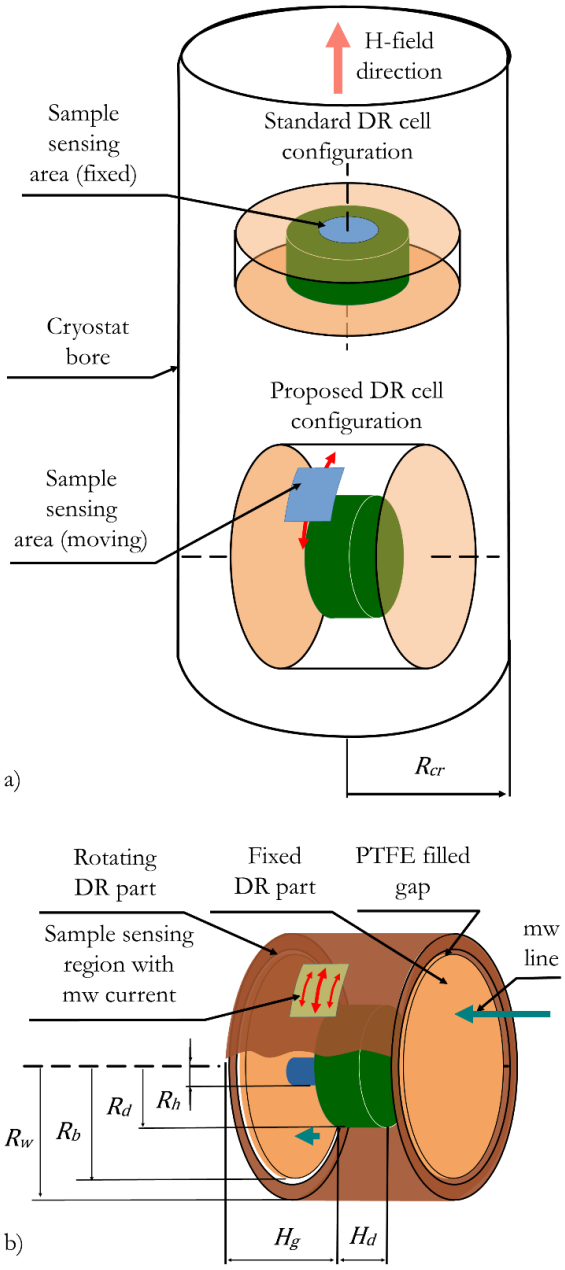

Figure 1. Draft of the DR cell. a) sketch of the DR cell inside a magnet bore. b) Draft of the DR cell with the two parts, the fixed one with the dielectric puck and the rotating one with the sample holder.

$$S_{R_S} = \left|\frac{\partial Q}{\partial R_S}\right| = \frac{Q^2}{G_S}, S_{X_S} = \left|\frac{\partial \Delta f_0}{\partial X_S}\right| \propto \frac{f_{0,\mathrm{ref}}}{2G_S}, \quad (2)$$

where $f_{0,\mathrm{ref}}$ is the reference frequency near f_0.

In standard configurations the static magnetic field is applied parallel to the resonator axis, and hence normal to the sample surface (see Figure 1a). In order to study the material anisotropic response to the orientation of the applied magnetic field, two possible approaches can be used: either rotate the magnet around the measuring cell or rotate the whole measuring cell within a fixed magnet. In the first case, specific magnets must be used, rotating either mechanically or magnetically. The added complexity makes them more expensive and limited in the maximum field attainable. The rotation of the whole cell, on the other hand, is hindered by the connection cables, given mainly by the microwave (mw) lines connecting the resonator to a microwave source and detector, which must be fixed.

Here we present for the first time a proof of concept based on a third path: a DR based measuring cell designed with a mobile part hosting the flat sample to be measured in various field orientations. To this purpose, in this novelty approach the sample would replace a portion of the lateral (curved) cavity wall [12].

2. DESIGN

The here presented concept is based on the standard approach for the Z_S measurement by means of DR, whereas several additional constraints are considered to achieve the stated goal.

First, the measuring cell with all its components and connectors should fit the bore of standard cryomagnets, which for hosting high field magnets have typical radii R_{cr} no larger than ~ 32.5 mm. Second, the DR must be able to operate in the ≤ 30 GHz range, where both the characteristic frequency of the materials to be studied and the operating frequencies of the mentioned applications are located [13], [14].

2.1. Definition of the DR geometry

The small sample space and the necessity to insert moving parts and cables are the main constraints on the DR cell design. A small cell size in turn leads to the higher resonant frequencies of DR.

In order to define the design framework, we first choose the DR resonant mode as a Transverse Electric TE_{0m1} mode, where m = 1, 2 .... Indeed, it is well-known that the TE_{011} mode has one of the lowest resonant frequencies with good enough frequency separation from other modes [6]. Moreover, all TE_{0m1} modes induce circular currents both on the bases and on the lateral wall of the cylindrical cavity. Hence, no current paths cross the base-wall boundary allowing to physically separate the bases from the wall without disrupting the resonance. This feature will prove extremely valuable in the forthcoming design process. Moreover, it has been shown that multifrequency measurements of the surface impedance are of great interest in the study of superconductors [15], [16]. Hence, this becomes an additional design goal, so we choose the TE_{021} mode as a second operating mode, since it shares (same third index) the same longitudinal configuration and thus induces the same current pattern on the lateral wall. This mode is similar to TE_{011} but is characterized by two peaks of electric field distribution along cavity radius. Using both TE_{011} and TE_{021} modes allows having a similar distribution of the induced microwave (mw) currents on the outer wall surface. Moreover, the TE_{0m1} modes induce the maximum current density at the middle plane of the dielectric puck.

The draft of the DR cell is shown in Figure 1b. The main idea is to conceive the DR cell as composed by two parts. The fixed part consists of the dielectric puck and flat circular bases, while the lateral wall of the resonant cavity becomes a moving, rotating part. The sample is fixed on the moving part, at the dielectric puck's mid-height level, where the induced currents are maximum in order to minimize the sample geometrical factor. This positioning allows obtaining maximum sensitivity on Z_S, see Equation (2), and, moreover, linear microwave currents on the sample surface. This is opposed to the circular current pattern encountered in the standard DR setup which, once used with tilted fields, determine non-homogeneous angles between field

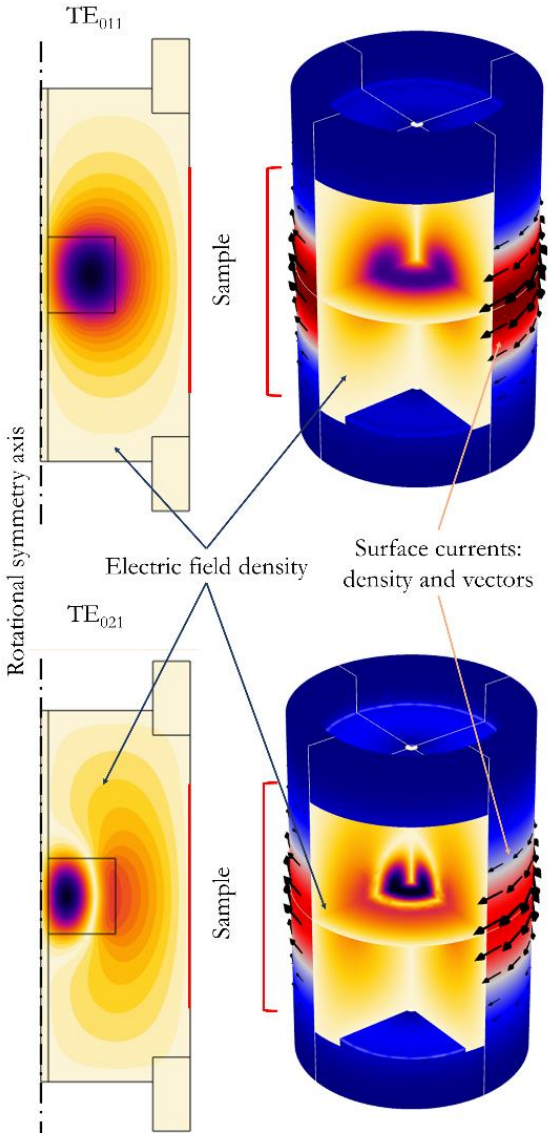

Figure 2. An example of the simulated TE_{011} and TE_{021} modes electromagnetic fields, in terms of their electric field spatial intensities (darker regions correspond to higher intensity) and induced surface current densities. The red line represents the sample sensing area. Black vectors represent surface currents.

and currents on the sample surface and ultimately hindering an anisotropy investigation [17].

To place the sample in the rotating part, a recessed blind hole, covered by a thin metallic mask with a rectangular slot, can be made in the lateral wall. In this way, the sample would not protrude in the cavity interior, and only a regular portion of its surface would be exposed to the microwave electromagnetic fields. In this preliminary design, we do not consider the details of mechanical supporting parts. To maintain a constant distance between the fixed resonator bases and the freely rotating lateral wall, we incorporate a thick PTFE layer between the parts. This gap does not affect the TE_{0m1} modes electromagnetic fields, which are concentrated near the dielectric puck, nor the current pattern induced in the enclosing surfaces, and thus minimally influences the characteristics of the DR cell.

The main components of the DR cell are represented in Figure 1b: the dielectric puck is placed coaxially to the cavity, between the two flat bases, and has radius R_b smaller than the wall radius R_w. We put (symmetrical) gaps H_g between the dielectric puck and the bases, so that power dissipation on the bases is reduced.

The dielectric puck can be fixed by dielectric supports attached to bases and puck. Here we considered to fix the dielectric with a dielectric tube or rod made from low-loss material inserted in the axial hole in the dielectric puck. This configuration allows to ensure mechanical stability of DR cell within a restricted space.

The coupling ports between the DR and microwave lines are placed on the fixed bases (see Figure 1b), instead of the usual coupling configuration protruding the lateral wall, since the latter is a moving part in the present design.

2.2. Definition of the size ranges

We performed an optimization of the size of the DR cell focusing on the sensitivity of the resonator response on R_S of the sample. The size starting value is given by the cryomagnet bore: considering the smaller values - encountered in high field ($\sim$ 10 T magnets), we set an upper limit for the external size of the whole cell to R_{cr} = 22.5 mm. Considering that the main part of the DR cell volume will consist in structural supporting parts, together with semi-rigid cryogenic coaxial cables, basic estimations yield the maximum external size of the cylinder, 31 mm. Indeed, the structural cavity parts should be at least 5 mm thick. Adding the space needed for coaxial cables ($\sim$5 mm), the internal cavity wall radius R_w is $\leq$ 10 mm, and analogously the corresponding maximum cavity height is $\leq$ 20 mm.

A first simulation of the simple Hakki-Coleman DR structure [18] allowed determining the optimal ratio 0.98 between the dielectric puck radius R_d and height H_d to yield a TE_{011} mode well isolated in frequency from spurious modes. For the present design, which involves a gapped structure and a second resonant mode, a possible different optimal value for R_d/H_d has been sought in a range centered in 0.98 mm. Based on the previous study [19] of the hollowed DR we consider $R_h = R_d/10$ so that to be much lower than $R_d/3$ where TE_{011} mode characteristics are independent on the presence of the hole.

The choice of the dielectric puck material is of paramount importance. Dielectrics with medium-high real permittivity ε_r are useful since they concentrate more the electromagnetic field within the dielectric puck and thus minimize the disrupting effects of the DR cell inhomogeneities and reduce eventual radiation. At cryogenic temperatures, single crystal sapphire is usually chosen due to its very low dielectric loss tangent and medium ε_r. In the following we considered relative permittivity parallel ($\varepsilon_r^{\parallel}$) and normal ($\varepsilon_r^{\perp}$) to the crystal main anisotropy axis $\varepsilon_r^{\parallel}$ = 11.59, $\varepsilon_r^{\perp}$ = 9.39 for temperature T = 295 K and $\varepsilon_r^{\parallel}$ = 11.35, $\varepsilon_r^{\perp}$ = 9.26 for temperature T = 50 K [20]. Loss tangent was taken to be $\tan\delta = 6.1 \times 10^{-6}$ for T = 295 K and $\tan\delta = 2.2 \times 10^{-8}$ for T = 295 K. Thus, reducing temperature, we expect even higher Q factors and relatively small growth of f_0.

Other higher ε_r materials, such as rutile, could be used to reduce the cavity size and/or resonant frequency, but with the drawback of a decreased Q and corresponding sensitivity. Specific investigations in this direction could be considered in future studies.

Since DR operates in the high magnetic field in cryogenic environments all its metallic parts should be nonmagnetic and should have a high thermal conductivity. For the following, we considered a medium-quality copper with R_S = 33.1 mΩ and

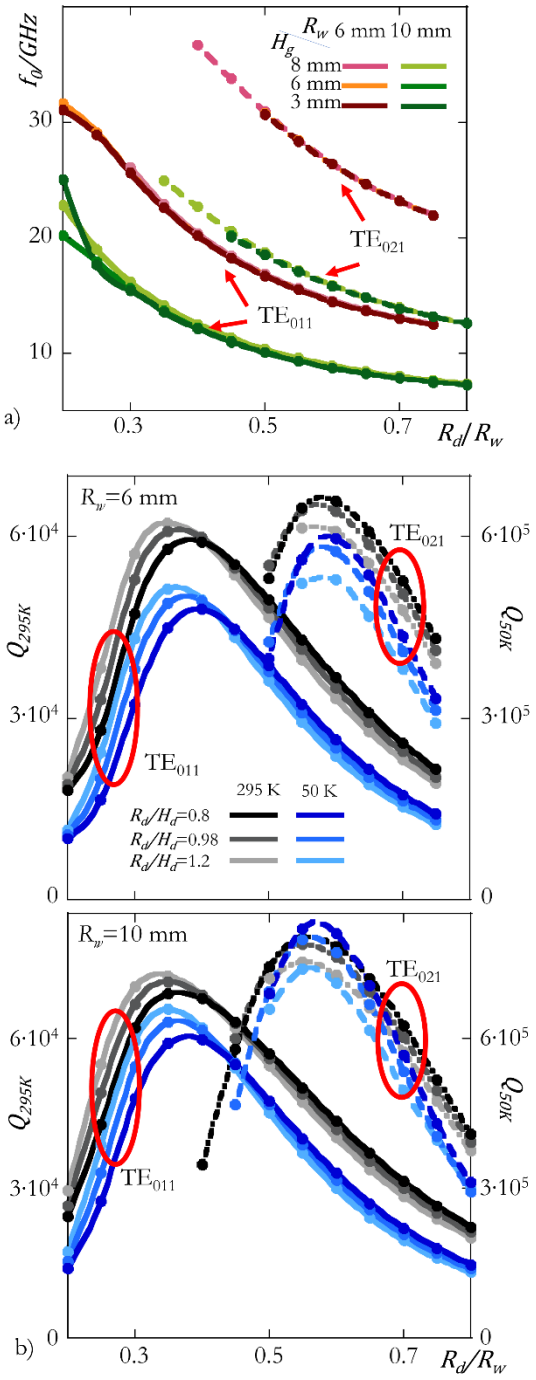

Figure 3. f_0 as a function of gap and cavity size (a) vs the normalized size of dielectric puck R_d/R_w. Q-factor (b) vs R_d/R_w, different R_d/H_d, R_w and H_g = 6 mm. All experimental dependencies represented for temperature 50 K and 296 K.

R_S = 5.8 mΩ (at f_0 = 16.8 GHz) at 295 K and 50 K correspondingly for all metallic parts of DR. To investigate the capabilities of the proposed DR cell we performed a full-wave Finite Element Method (FEM) simulation. A 3D simulation of the detailed resonator structure needs large calculating power and thus is inefficient in the initial stages of the design process. Hence, in the following we present the results of a 2D (axisymmetric) model, made possible by the axisymmetry of both the DR structure and of the chosen TE_{0m1} modes.

3. DISCUSSION

The FEM simulation was performed taking into account the material properties, for both dielectrics and conductors, at variable temperature between 40 K and 300 K.

In Figure 2 we show an example of the used simulated axisymmetric model. For this 2D axisymmetric model, the sensing area is represented as a 10 mm-wide strip along the whole cavity wall circumference. Figure 2 illustrates a representative example of electric field distribution corresponding to the two modes under study. For future 3D simulation and real DR, samples will be only a small portion of this strip as shown in Figure 1b.

As anticipated in the previous Section, the optimization of the DR cell size is done by taking a fixed ratios R_d/H_d in the range near 0.98 (R_d/H_d = 0.8 – 1.2). The symmetrical gap between dielectric puck and bases H_g is varied in the range 0.1 mm – 9 mm. Since a small cavity radius is preferable, we studied also the effect of the cavity wall radius R_w by varying it between 6 mm and 12 mm. Given the circular shape of the magnet bore, analogous limits hold also for the longitudinal direction of the DR cell, being $H_d + 2H_g$ its total height (see Figure 1b). As a result, the investigated parameters space is: R_d/H_d = 0.8 – 1.2, H_g = 0.1 mm – 9 mm, R_w = 3 mm – 12 mm. Since this multi-variable space of parameters is large, here we focus on selected results.

For each parameters set, the resonant modes were calculated using eigenmode e.m. solver and all resonant parameters. The TE_{011} and TE_{021} modes were identified from other modes using an automatic script which detects the maxima, minima and lobes in the field spatial distributions to identify the mode type and indexes. Upon increasing the dielectric puck size R_d/R_w from 0.2 to 0.8, the Q factors exhibit a maximum whose position slightly shifts, for both modes, by increasing the gap H_g from 3 mm to 10 mm. f_0 reduces drastically with R_d/R_w and additionally it can be decreased by increase of H_g and R_w (see Figure 3a). Independently from the dielectric puck size R_d/H_d and from the cavity size R_w, even for small gaps H_g above 3 mm, the maxima of $Q(R_d/R_w)$ are in the same R_d/R_w, albeit different for the two modes (R_d/R_w = 0.3 − 0.5 and R_d/R_w = 0.5 − 0.7 for TE_{011} and TE_{021}, respectively). It should be noted that the positions of these maxima persist in the whole temperature range studied (Figure 3b) despite the higher Q by one order of magnitude at 50 K. This implies that a simultaneous optimization for both modes is not possible, but a trade-off must be sought. In those regions of R_d/R_w adding the gap up to 6 mm one could obtain 10-times higher Q for TE_{011} and 5-times higher Q for TE_{021}. Considering the intersection of optimal Q regions for both modes, R_d/R_w = 0.45 − 0.55 can be chosen.

Although Q is an important parameter for the sensitivity on R_S, also the geometrical factor of the sensing region (G_S,) contributes, see Equation (2). Analyzing the sensitivity, it can be seen that $S_{R_S}(R_d/R_w)$ is also characterized by a peak (see Figure 4). As in the case of Q, by increasing the gap, the S_{R_S} maximum moves to lower R_d/R_w values and does not change visibly above H_g = 6 mm. Maximum R_S sensitivity at large gap can be obtained for dielectrics with R_d/R_w = 0.4 and R_d/R_w = 0.6 for TE_{011} and TE_{021} modes, respectively. An opposite situation occurs for the sensitivity on X_S, $S_{X_S}(R_d/R_w)$ has a minimum where S_{R_S} is maximum. The choice of the

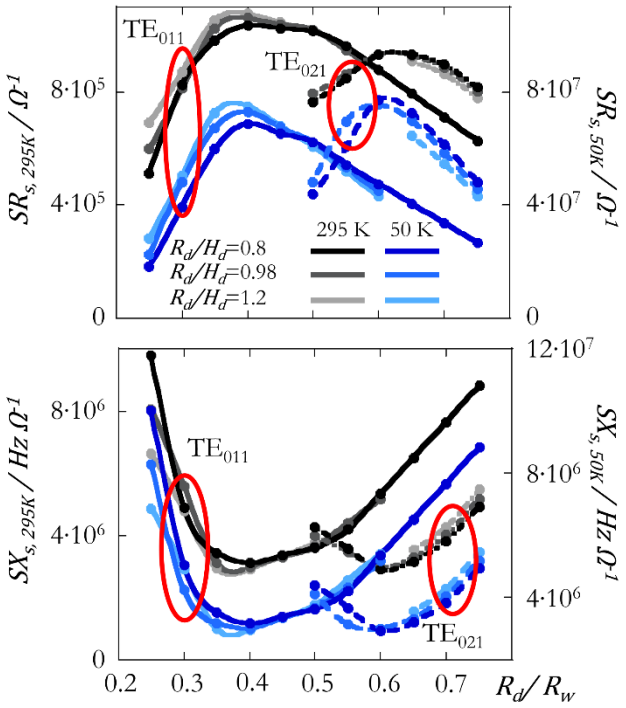

Figure 4. Sensitivity of the resonator on R_S and X_S as a function of dielectric puck size for TE_{011} and TE_{021} modes, different R_d/H_d values, R_w = 6 mm and different resonator temperatures (50 K and 295 K) H_g. Cavity height is kept below 20 mm and modes separated by 10.5 GHz from spurious modes.

optimal geometry for both R_S and X_S becomes challenging. One is forced to choose the DR cell dimensions out of optimal S_{R_S} to achieve a sufficient sensitivity also on X_S. It should be noted that $\max(S_{R_S})$ and $\min(S_{X_S})$ positions are independent on the ratio R_d/H_d between 0.8 and 1.2.

Even considering such a complex set of parameters to optimize the band $R_d/R_w = 0.45 - 0.55$ could be considered as optimal both for simultaneous measurement of R_S and X_S cand for the use of two TE_{0m1} modes in the temperature range between 50 K and room temperature.

We used additional criteria to find an optimal gap and cavity wall radius: the operating mode should be at least 0.5 GHz distant from spurious ones in the frequency spectrum and the sensitivity on sample impedance S_{Z_S} should be at least 5 times higher than the sensitivity on base impedance. We noted that for relatively small H_g or for large cavity R_w the DR cell could not satisfy the sample S_{Z_S} criterium, while large gap H_g could produce a denser frequency spectrum. Small cavity R_w leads to high resonant frequencies, in particular, TE_{021} modes f_0 could be above 30 GHz criterium. We determine H_g near 6 mm and R_w near 6 mm as optimal.

Summarizing, the DR geometry yielding an optimal dual-mode sensitivity is: $R_d/H_d = 0.5$, $H_g = 6$ mm and $R_w = 6$ mm. An estimation of the minimum detectable R_S variation ($\Delta R_S = \min(Q)/S_{R_S}$) can be done considering a minimum detectable $\min(Q) = 40$ and a realistic size for the sample. Taking for the latter a rectangle 10 mm wide and $\ell = 6$ mm long, it would cover a fraction $\ell/(2\,\pi\,R_w) = 0.16$ of the lateral wall circumferences with a proportional reduction on the sensitivity. Thus, one obtains $\Delta R_S = 0.24$ mΩ and $\Delta R_S = 0.30$ mΩ for TE_{011} and TE_{021}, respectively at $T = 295$ K. Decreasing temperature of the cell down to 50 K we observe nearly two order of magnitude higher S_{R_S}. This corresponds to the lower ΔR_S: $\Delta R_S = 4.0$ μΩ and $\Delta R_S = 5.2$ μΩ for TE_{011} and TE_{021}.

4. CONCLUSIONS

We have proposed a concept of a DR-based measuring cell for the measurement of the surface impedance of superconducting samples in magnetic fields with varying orientations. The proposed measuring cell consists in a DR divided in two parts. A fixed one includes the dielectric puck and the bases. The second one, given by the lateral wall, is conceived to accommodate the sample and to be able to rotate within a fixed magnetic field. The main design goals and constraints have been identified and tackled with. A preliminary study, with FEM simulations, allowed to identify the ranges for the resonator dimensions needed to optimize the sensitivity on Z_S measurements. A potential minimum detectable ΔR_S for measurements on 10 mm-wide and $\ell = 6$ mm long samples at frequencies near 16.75 GHz and 30.8 GHz is expected to decrease cooling from room to 50 K from $\Delta R_S = 0.24$ mΩ to $\Delta R_S = 4.0$ μΩ for TE_{011} and from $\Delta R_S = 0.30$ mΩ to $\Delta R_S = 5.2$ μΩ for TE_{021}.

REFERENCES

[1] P. Wikus, W. Frantz, R. Kummerle, P. Vonlanthen, Commercial gigahertz-class NMR magnets, Supercond. Sci. Technol., 35 (2022) Art. Id. 033001.
DOI: 10.1088/1361-6668/ac4951

[2] A. E. Costley, Towards a compact spherical tokamak fusion pilot plant, Philosophical Transactions of the Royal Society A: Mathematical, Physical and Engineering Sciences, 377 (2019) Art. Id. 20170439.
DOI: 10.1098/rsta.2017.0439

[3] S. Calatroni, HTS Coatings for Impedance Reduction in Particle Accelerators: Case Study for the FCC at CERN, IEEE Trans. Appl. Supercond., 26 (2016) Art. Id. 3500204.
DOI: 10.1109/TASC.2016.2520079

[4] D. Alesini, C. Braggio, G. Carugno (+ 22 more authors), Galactic axions search with a superconducting resonant cavity, Phys. Rev. D, 99 (2019) Art. Id. 101101(R).
DOI: 10.1103/PhysRevD.99.101101

[5] International Electrotechnical Commission, IEC 61788-7:2020 Superconductivity – Part 7: Electronic characteristic measurements - Surface resistance of high-temperature superconductors at microwave frequencies, 2020, p. 87.

[6] A. Alimenti, K. Torokhtii, E. Silva, N. Pompeo, Challenging microwave resonant measurement techniques for conducting material characterization, Meas. Sci. Technol., 30 (2019).
DOI: 10.1088/1361-6501/ab0e65

[7] N. Pompeo, K. Torokhtii, A. Alimenti, E. Silva, A method based on a dual frequency resonator to estimate physical parameters of superconductors from surface impedance measurements in a magnetic field, Measurement, 184 (2021).
DOI: 10.1016/j.measurement.2021.109937

[8] B. W. Hakki, P. D. Coleman, A Dielectric Resonator Method of Measuring Inductive Capacities in the Millimeter Range, IRE Trans. Microw. Theory Tech., 8 (1960) pp. 402-410.
DOI: 10.1109/TMTT.1960.1124749

[9] L. F. Chen, C. K. Ong, C. P. Neo, V. V. Varadan, V. K. Varadan, Microwave Electronics: Measurement and Materials Characterization, Wiley, 2004, ISBN: 978-0-470-84492-2.

[10] N. Pompeo, K. Torokhtii, E. Silva, Dielectric resonators for the measurements of the surface impedance of superconducting films, Meas. Sci. Rev., 14 (2014) pp. 164–170.
DOI: 10.2478/msr-2014-0022

[11] A. Alimenti, K. Torokhtii, N. Pompeo, E. Piuzzi, E. Silva, Microwave Characterization of 3D-printer Dielectric Materials, Proc. 23rd IMEKO TC4 Int. Symp. electrical & electronic measurements promote industry 4.0, Xi'an, China, 17-20 September 2019. Online [Accessed 22 September 2023] https://www.imeko.org/publications/tc4-2019/IMEKO-TC4-2019-021.pdf

[12] K. Torokhtii, A. Alimenti, N. Pompeo, E. Silva, Surface resistance scanner of the irregular pipe structures, Proc. 24th IMEKO TC4 International Symposium, Palermo, Italy, 14-16 September 2020. Online [Accessed 22 September 2023] https://www.imeko.org/publications/tc4-2020/IMEKO-TC4-2020-14.pdf

[13] A. Alimenti, N. Pompeo, K. Torokhtii, E. Silva, Surface Impedance Measurements in Superconductors in DC Magnetic Fields: Challenges and Relevance to Particle Physics Experiments, IEEE Instrumentation and Measurement Magazine, 24 (2021) pp. 12–20, Dec. 2021. DOI: 10.1109/MIM.2021.9620046

[14] A. Alimenti, K. Torokhtii, D. Di Gioacchino, C. Gatti, E.Silva, and N. Pompeo, Impact of Superconductors Properties on the Measurement Sensitivity of Resonant-Based Axion Detectors, Instruments, 6 (2021). DOI: 10.3390/instruments6010001

[15] A. Alimenti, K. Torokhtii, P. Vidal García, E. Silva, M. A. Grigoroscuta, P. Badica, A. Crisan, N. Pompeo, Measurements of Surface Impedance in MgB2 in DC Magnetic Fields: Insights in Flux-Flow Resistivity, Materials, 16 (2023). DOI: 10.3390/ma16010205

[16] N. Pompeo, K. Torokhtii, A. Alimenti, G. Sylva, V. Braccini, E. Silva, Pinning properties of FeSeTe thin film through multifrequency measurements of the surface impedance, Supercond. Sci. Technol., 33 (2020) Art. Id. 114006. DOI: 10.1088/1361-6668/abb35c

[17] N. Pompeo, E. Silva, Analysis of the Measurements of Anisotropic AC Vortex Resistivity in Tilted Magnetic Fields, IEEE Trans. Appl. Supercond., 28 (2018) Art. Id. 8201109. DOI: 10.1109/TASC.2018.2797258

[18] K. Torokhtii, N. Pompeo, S. Sarti, E. Silva, Study of cylindrical dielectric resonators for measurements of the surface resistance of high conducting materials, Proc. 22nd IMEKO TC4 International Symposium, Iasi, Romania, 14-15 September 2017. Online [Accessed 22 September 2023] https://www.imeko.info/publications/tc4-2017/IMEKO-TC4-2017-024.pdf

[19] K. Torokhtii, N. Pompeo, E. Silva, Multifunctional Hollow Dielectric Resonator Design for Conductivity/Permittivity Measurements of Bulk Samples, Proc. 22nd IMEKO TC4 International Symposium, Iasi, Romania, 14-15 September 2017. Online [Accessed 22 September 2023] https://www.imeko.org/publications/tc4-2017/IMEKO-TC4-2017-025.pdf

[20] J. Breeze, Temperature and frequency dependence of complex permittivity in metal oxide dielectrics: Theory, modelling and measurement, 1st ed. Basel, Switzerland: Springer International Publishing, 2016, ISBN: 978-3-319-44547-2.